УДК 621.314.1 DOI: https://doi.org/10.15407/techned2026.03.021

LOAD-DEPENDENT CONTROL OF BIDIRECTIONAL DC-DC CONVERTERS FOR HEAVY DUTY LOADS

S.P. Peresada[1*], Ye.O. Nikonenko[1], S.Ye. Lyshevski[2***]**
[1] National Technical University of Ukraine "Igor Sikorsky Kyiv Polytechnic Institute",
37, Beresteiskyi Ave., Kyiv, 03056, Ukraine, e-mail: sergei.peresada@gmail.com.
[2] Rochester Institute of Technology,
Rochester, NY, USA.

The paper presents design of cascaded DC-link voltage control systems for bidirectional buck-boost DC-DC converters which supply high dynamic loads such as IPMSM electrical drives. A new design methods applied for class of commutated DC-DC converters, which known as strongly nonlinear and non-minimum-phase plants, improved not only their dynamic performance but defined a new system features and therefore new opportunities for their further development and optimization. Control algorithm based on PI current and voltage controllers forms the composite system which consists of two linear stable subsystems in a nonlinear feedback loop suitable to apply the theory of cascaded systems with two time-scale separation of the control loops dynamics. As it follows from the analysis after linearization, the load current acts not only as external disturbance but defines closed loop systems parameters as well, and consequently their dynamics and stability. To overcome this problem the combination of two technologies has been proposed for controller design: a) "symmetrical" like optimum with worst-case system tuning in order to preserve system stability margin depending on maximum values of loads; b) disturbance rejection technique to improve accuracy of voltage regulation on the base of direct load current measurement or estimation. Two technologies do not contradict each other since later one is an intrinsically open loop. When DC-DC converter is used as power supply of vector controlled drives the required load information is computed from the power balance equation of complete electromechanical system 'DC-DC converter – electrical drive'. The composite electromechanical system ensures high dynamic performance and extended power capability of the DC-DC converter, which is confirmed by the results of experimental tests and simulation study based on experimental transients of the electrical drive. References 13, Fig. 7, Table 1.
***Keywords**:* DC-DC buck-boost converter, control algorithm, electrical drives, voltage controller, stability, load current compensation.

Introduction. Bidirectional DC-DC buck-boost converters (also known as two-quadrant converters) are widely applied in electric vehicles, energy storage systems, power sources etc. in order to regulate the output DC-link voltage [1, 2]. The control systems of DC-DC power converters must provide the specified dynamic performance and stability properties with respect to 'heavy' variations of load current, including those that are close to critical values, defined by the power balance equation [3, 4]. The control problem is further complicated by significant nonlinearity and non-minimum-phase nature of the converter model due to presence of the right-half-plane roots of the linearized model characteristic equation.

Since 1990s, the DC-DC and AC-DC converters established a class of controlled plants known as "switching power converters". The control theory of such systems was developed in a significant number of fundamental and technical studies which are summarized in [1 – 5] (see references therein). Variety of methods, based on classical control theory and advanced methods of modern nonlinear control using the consideration of both, converter averaged coordinates [6] and its instantaneous values, have been proposed by both theoretically and technically oriented control societies. Many modern solutions, for example, model predictive control [7], allow to achieve high dynamic performance, but the dynamic behavior is difficult to specify during controller design. The algorithms, designed using passivity-based control technique [5] and second Lyapunov method [8, 9], do not provide predefined dynamic performance as well. In [10] it is shown that nonlinear DC-DC model is feedback linearizable in energy-based state-space (total system energy and instantaneous power). The resulting dynamic system is linear and stable provided that constraints of the power balance equation are satisfied. Such feedback linearizing controller cannot be implemented in practice since

ORCID: * https://orcid.org/0000-0001-8948-722X; ** https://orcid.org/0000-0003-2379-5566;
*** https://orcid.org/0000-0003-1340-4824

the exact parameters of the energy storage elements (DC-link capacitance and input circuit inductance) are needed to compute the regulated energy. Only a few control methods provide the effective inductor current limitation.

As it follows from the literature analysis and a practical viewpoint, the most widespread approach is application of state feedback control structure, which consists of cascaded current and voltage control loops having different modifications of proportional-integral (PI) controllers. They, de-facto known as 'standard' systems, are sufficiently robust, provide effective internal variables limitation, and relatively simple in implementation. For the most algorithms, controller design and analysis are based on simplifying assumptions due to complexity of significant nonlinearity and non-minimum-phase nature of the converter model. Such approach gives quite satisfactory results for load currents, which are relatively small, compared to power balance critical values.

In the first part of this research [11], authors proposed new design and analysis of the DC-DC converter cascaded control system, which is based on partial feedback linearization and two-time scale decomposition leading to special nonlinearly interconnected structure of the two linear asymptotically stable systems in a feedback loop As a result, linearized system shows that load current acts not only as an external perturbation but also changes parameters of the closed-loop system, defining in such way stability margin and transient performance. This feature opens perspectives for improving the overall control algorithm using load current information for implementation of available control techniques to stabilize system dynamics and compensate disturbances. The focus of this research is primarily oriented on power DC-DC converters, where suitable dynamic performance and extended stability range with respect to heavy load currents are required, for example, to supply the electric vehicle (EV) drive systems based on vector-controlled IPMSM.

The aim of this paper is to develop a novel, load current dependent control algorithm for cascaded control systems of the bidirectional DC-DC buck-boost converters supplying the high dynamic active loads to ensure improved system dynamic performance and extended load current range.

DC-DC buck-boost converter control. A standard schematic diagram of the DC-DC converter is shown in Fig. 1, where V_{dc} and i are DC-link voltage and input current; i_L is load current; L, R – input circuit inductance and internal resistance; E is power supply voltage; C – output capacitance; $Q, \overline{Q}$ – control signals of the switches. It is assumed that all electrical elements are linear, parameters are constant, transistors are ideal, which are turned on/off in a complementary way maintaining DC-link voltage at a reference level.

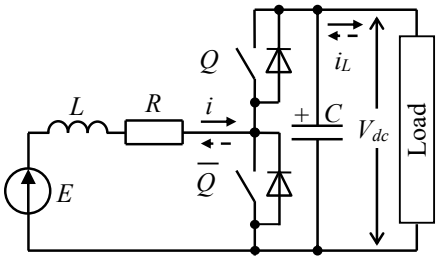

Fig. 1

Mathematical model of DC-DC converter is [1]

$$\begin{aligned} \dot{z} &= \frac{2}{C}\left(\left[1-u_{sw}\right]V_{dc}i - V_{dc}i_L\right), \\ \dot{i} &= \frac{1}{L}\left(-Ri - \left[1-u_{sw}\right]V_{dc} + E\right), \end{aligned} \tag{1}$$

where $z = V_{dc}^2$, and the switching function is defined as

$$u_{sw} = \{0,1\}. \tag{2}$$

The controlled variable in (1) is the square of DC-link voltage z, the control action is the switching function u_{sw}, and the load current i_L is the disturbance. The model (1), (2) is nonlinear and non-minimum-phase [5]. The control action u_{sw} is a discontinuous function formed as a PWM-signal. Under conditions of correctly selected switching frequency, the model in averaged coordinates [6] is equal to

$$\begin{aligned} \dot{z} &= \frac{2}{C}\left(ui - V_{dc}i_L\right), \\ \dot{i} &= \frac{1}{L}\left(-Ri + E - u\right), \end{aligned} \tag{3}$$

where

$$u = (1-u_{sw})V_{dc}, \tag{4}$$

and u_{sw} is a continuous in time and bounded signal.

Consider model (3) and the following assumptions.

A.1. Reference voltage and input voltage: $V_{dc}^* > 0$, $V_{dc}^* = const$, $E > 0$, $E = const$, $z^* = V_{dc}^{*2} = const$.

A.2. All parameters are known and constant, i_L = const.

A.3. Input current i and voltage E, and DC-link voltage V_{dc} are available for measurements.

Under condition of these assumptions, it is required to design a control algorithm which guarantees asymptotic voltage regulation, i.e.

$$\lim_{t\to\infty}\tilde{z}=0\,,\ \tilde{z}=z-z^*\,, \tag{5}$$

where $\tilde{z}$ is the DC-link voltage regulation error.

Voltage and current control. The nonlinear transformations $z=V_{dc}^2$ and $u=(1-u_{sw})V_{dc}$ in (4) perform the first step in partial feedback linearization of the DC-DC converter dynamic model.

Following the cascaded systems design procedure, we construct the linear PI current controller as

$$\begin{aligned} &u=E-Ri^*+\upsilon, \qquad \upsilon=L(k_{i1}\tilde{i}+k_{ii}x_i),\\ &\dot{x}_i=\tilde{i}\,, \end{aligned} \tag{6}$$

where $\tilde{i}=i-i^*$ is the current regulation error; i^* is the reference current (output of the voltage controller); (k_{i1}, k_{ii}) > 0 are the proportional and integral gains of the current controller.

Substituting (6) into second equation of (1) the resulted current error dynamics is given by

$$\begin{aligned} &\dot{x}_i=\tilde{i}\,,\\ &\dot{\tilde{i}}=-k_i\tilde{i}-k_{ii}x_i-\dot{i}^*, \end{aligned} \tag{7}$$

where $k_i = k_{i1} + R/L$.

Controller (6) provides compensation of the time constant L/R in the 2nd equation of (1) if controller tuning is selected as $Lk_{ii} = R/\tau_i$, $k_{i1} = 1/\tau_i$, where τ_i is current control loop time constant. The resulting current loop dynamics is reduced to

$$\dot{\tilde{i}}=-\frac{1}{\tau_i}\tilde{i}-\dot{i}^*. \tag{8}$$

From the definition (5) and $\tilde{V}_{dc}=V_{dc}-V_{dc}^*$, it goes that

$$\tilde{V}_{dc}=\frac{\tilde{z}}{V_{dc}+V_{dc}^*}\,,\ V_{dc}i_L=\frac{\tilde{z}}{V_{dc}+V_{dc}^*}i_L+V_{dc}^*i_L\,,\ V_{dc}^*i_L=\text{const}\,.$$

Taking into account (6), voltage dynamics becomes

$$\dot{\tilde{z}}=\frac{2}{C}\left(-\frac{i_L}{V_{dc}+V_{dc}^*}\tilde{z}+\left(E-Ri^*+\upsilon\right)\left(i^*+\tilde{i}\right)-V_{dc}^*i_L\right). \tag{9}$$

Since $(E - Ri^*) \approx E > 0$, a linear PI-voltage controller can be designed from (9) as [11]

$$\begin{aligned} &i^*=\frac{C}{2}\frac{1}{E}\left(-k_v\tilde{z}-k_{vi}x_v\right),\\ &\dot{x}_v=\tilde{z}, \end{aligned} \tag{10}$$

where (k_v, k_{vi}) > 0 are the proportional and integral gains of the voltage controller.

Combining (7), (9), (10) the resulting voltage-current dynamics is given by

$$\begin{aligned} &\dot{x}_v=\tilde{z},\\ &\dot{\tilde{z}}=-\left(\frac{2}{C}\frac{1}{V_{dc}+V_{dc}^*}i_L+\frac{E-Ri^*}{E}k_v\right)\tilde{z}-\frac{E-Ri^*}{E}k_{vi}x_v+\frac{2}{C}\left(\upsilon i^*+(E-Ri^*+\upsilon)\tilde{i}-V_{dc}^*i_L\right), \end{aligned} \tag{11}$$

$$\begin{aligned} &\dot{x}_i=\tilde{i}\,,\\ &\dot{\tilde{i}}=-k_i\tilde{i}-k_{ii}x_i-\dot{i}^*, \end{aligned} \tag{12}$$

where $\upsilon = L(k_{i1}\tilde{i}+k_{ii}x_i)$, $(2/C)i_L/(V_{dc}+V_{dc}^*)+k_v(E-Ri^*)/E>0$.

System dynamics analysis and controller parameters tuning. Nonlinear non-minimum-phase systems (11) and (12) describe dynamic behavior of the voltage and current control loops and present a nonlinear feedback-interconnection of the two linear asymptotically stable systems (in the isolated state). Stability analysis and dynamic performance specification for the controller tuning of the composite system (11), (12) has been performed using two-time scale separation approach on the base of linearized dynamics. According to the theory of cascaded systems the inner current control loop should be at least several times faster than the outer voltage control loop [11].

Since inductor resistance is parasitic one, we consider system with $R = 0$ under no load condition $V_{dc}^*i_L=0$. Neglecting bilinear nonlinearities in (11) we obtain (for current controller tuning according to (8)):

$$\begin{aligned}\dot{x}_v &= \tilde{z},\\ \dot{\tilde{z}} &= -k_v\tilde{z} - k_{vi}x_v + \frac{2}{C}E\tilde{i},\\ \dot{\tilde{i}} &= -k_i\tilde{i}_i + \frac{C}{2}\frac{1}{E}\left(k_v\dot{\tilde{z}} + k_{vi}\tilde{z}\right).\end{aligned} \tag{13}$$

Linearized structure (13) allows to study stability of the equilibrium point $(x_v, \tilde{z}, \tilde{i}) = \mathbf{0}$ on the base of so-called "nominal" dynamics. The open-loop transfer function corresponding to (13) is equal to

$$W_{r1}(p) = \frac{(2\xi_v\tau_v p + 1)}{\tau_v^2 p^2}\cdot\frac{1}{(\tau_i p + 1)}, \tag{14}$$

where $\tau_v^{-2} = \omega_{0v}^2 = k_{vi}$, ω_{0v} is the frequency of the undamped oscillations of the isolated voltage control loop; $\omega_{0i} = \tau_i^{-1} = k_i$, $k_v = 2\zeta_v\omega_{0v}$, where ζ_v is the damping coefficient in the voltage control loop.

System dynamics described by the open-loop system transfer function (14) corresponds to the structure which allows tuning according to "symmetrical" like optimum with $\omega_{0i} = \rho\omega_{0v}$, $\rho \geq 2\sqrt{2} \div 4$ [11]. The standard tuning with $\zeta = 1$ $(k_{vi} = k_v^2/4)$ or $\zeta = \sqrt{2}/2$ $(k_{vi} = k_v^2/2)$ typically is used for 2nd-order isolated voltage loop dynamics with the characteristic frequencies of (14) are located at 2 octaves from the cutoff frequency. Important to note that "nominal" dynamics has well-defined dynamic performance and is robust to bounded parameter's perturbation.

If $i_L \neq 0$ but bounded the structure of (11), (12) is strongly nonlinear and can be viewed as "nominal" linear one (13), perturbed by load-dependent terms as follows from open-loop transfer function given by

$$W_r(s) = \frac{\left(2\xi_v\tau_v s + 1\right)\left[1 - \frac{L}{E^2}V_{dc}^* i_L s\right] + \left[\frac{1}{CV_{dc}^*}\tau_v^2 i_L s(\tau_i s + 1)\right]}{\tau_v^2 p^2(\tau_i s + 1)}. \tag{15}$$

Study [11] suggests to use condition $\rho > 2\sqrt{2}$ for the stability margin increase with respect to load perturbations. With such tuning there exists maximal value $i_{L\max}$ when linearized system (15) is asymptotically stable provided that load current $i_L \leq i_{L\max}$ and, therefore $(x_v, \tilde{z}, \tilde{i}) = \mathbf{0}$ is a locally asymptotically stable equilibrium point of the nonlinear system (11), (12). The importance of such representation is that the linearized system allows to define the influence of $V_{dc}^* i_L$ not only as external disturbance but also to assess its effect on the parameters of the closed-loop system. Therefore, the proposed presentation enables analysis of the impact of i_L on system stability and dynamic performance. For this purpose, a characteristic equation of the system (15) is convenient to present in the following form:

$$\tau_v^2\tau_i s^3 + \tau_v^2 k_2(i_L)s^2 + \tau_v^2 k_1(i_L)s + 1 = 0, \tag{16}$$

where $k_1(i_L) = k_v + i_L/(CV_{dc}^*) - Lk_{vi}V_{dc}^* i_L/E^2$, $k_2(i_L) = 1 + \tau_i i_L/(CV_{dc}^*) - Lk_v V_{dc}^* i_L/E^2$.

From the conditions $k_1(i_L) > 0$ and $k_1(i_L) > 0$ it follows that for fixed τ_i the voltage controller tuning parameters (k_v, k_{vi}) should be different for different values of load current.

The initial voltage control loop tuning is based on the standard "symmetrical optimum" for $i_L = 0$: $\omega_{0i} = \rho\omega_{0v}, \rho = 2\sqrt{2}, \zeta = \sqrt{2}/2$ with fixed desired (achievable) current loop dynamics, defined by $\omega_{0i} = \tau_i^{-1}$. As result of computation, the initial voltage controller gains are defined as: $k_v = 2\zeta_v\omega_{0v}$, $k_{vi} = \omega_{0v}^2$.

In case i_L = const or slowly varying, the direct adjustment of voltage controller gains (k_v, k_{vi}) as a function of measured i_L can be implemented in order to improve dynamic performance and increase the load capability as compared to standard "symmetrical optimum" tuning.

In contrast to most spread power supplies with constant loads, the control systems of EV battery supply should provide the suitable dynamic performance and extended stability range with respect to heavy and rapidly changing bidirectional load currents. In such systems maximum values of the load currents should be considered to define the "worst-case" tuning for $|i_L| \leq i_{L\max}, i_{L\max} = \text{const}$. One of possible approaches is to find the appropriate relation $k_v(i_{L\max})$ with $k_{vi}(i_{L\max}) = k_v^2(i_{L\max})/(2 \div 4)$ in order to set the same system stability margin under different load currents, for example, considering system Bode diagrams or other available techniques for linear systems with varying parameters.

Tuning example. The model parameters of the studied DC-DC converter are given in the Appendix A. Input voltage $E = 130$ V, $V_{dc}^* = 300$ V. Current controller is tuned at: $\tau_i^{-1} = \omega_{0i} = 1800$ rad/s.

Following the approach, leading to the same phase stability margin for different load currents, the required data are reported in Table, obtained from the Bode diagrams for $W_r(s)$ (15), shown in Fig. 2, *a*.

No. of test	1	2	3	4	5	6
Load current i_L, A	0	0.5	1	2	3	5
Proportional gain k_v	900	900	770	600	495	370
Cut-off frequency, rad/s	900	903	793	643	546	425
Phase stability margin, deg.	37	31	31	31	31	31

Transients for standard "symmetrical optimum" ($k_i = 1800$, $k_v = 900$) are depicted in Fig. 2, *b* for a set of load currents $i_L = [0.5, 3]$ A. Load current was applied at $t = 0.05$ s and removed at $t = 0.15$ s with limited rate of 1 A/ms. Note that the system is unstable for $i_L = 5$ A. Transients for the proposed tuning according to Table for $i_L \le i_{L\max} = 5$ A ($k_i = 1800, k_v = 370$), which are shown in Fig. 2, *c*, demonstrate stable operation for all currents $i_L \le i_{L\max}$.

Improved control with direct load compensation. The main limitation of the approach which considers voltage controller worst-case tuning depends on the robustification mechanism: for increased load current the cut-off frequency of the voltage control loop requires to be reduced in order to maintain the same phase stability margin. This leads to reduction of dynamic accuracy while quality of voltage transients remains almost the same (see Fig. 2, *c*).

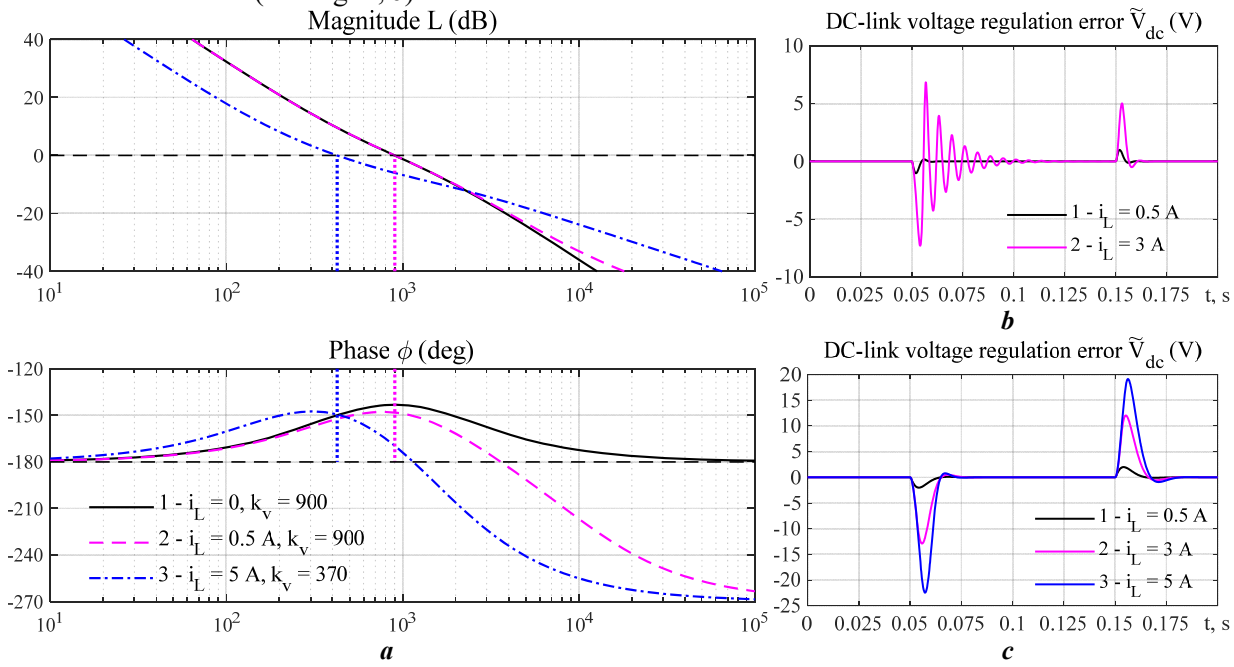

Fig. 2

In order to improve dynamic accuracy during load compensation by action of voltage controller with worst-case tuning we propose to apply disturbance compensation technique. The designed cascaded control system (11), (12) has physically based structure which forms regulation current by high-speed inner control loop according to power balance equation.

As it follows from equation (11) the load perturbation has physical meaning in the terms of output power $V_{dc} i_L$ according to power balance equation in steady-state $Ei - Ri^2 - V_{dc} i_L = 0$ and therefore current reference trajectories are computed as:

$$i_c^* = \frac{E - \sqrt{E^2 - 4RV_{dc}^* i_L}}{2R}.$$

The modified dynamic voltage controller with load compensation component is constructed on the base of (10) as follows ($R = 0$):

$$\begin{aligned} i^* &= \frac{C}{2}\frac{1}{E}\left(-k_v \tilde{z} - k_{vi} x_v\right) + \frac{1}{E}\xi, \\ \dot{x}_v &= \tilde{z}, \\ \dot{\xi} &= -\tau_f^{-1}\xi + \tau_f^{-1}(V_{dc}^* i_L), \end{aligned} \qquad (17)$$

where ξ is filtered load compensation component; τ_f is the a small time constant of low-pass filter to limit

signals derivatives and to adjust speed of load compensation.

Dynamics of the voltage and current errors with controller (17) can be written as ($R = 0$):

$$\begin{aligned}
&\dot{x}_v = \tilde{z},\\
&\dot{\tilde{z}} = -\left(\frac{2}{C}\frac{1}{V_{dc}+V_{dc}^*}i_L + k_v\right)\tilde{z} - k_{vi}x_v + \frac{2}{C}\xi + \frac{2}{C}\left(\upsilon i^* + (E+\upsilon)\tilde{i} - V_{dc}^* i_L\right),\\
&\dot{\xi} = -\tau_f^{-1}\xi + \tau_f^{-1}(V_{dc}^* i_L),\\
&\dot{\tilde{i}} = -\frac{1}{\tau_i}\tilde{i} + k_v\dot{\tilde{z}} + k_{vi}\tilde{z} - \frac{1}{E}\left(-\tau_f^{-1}\xi + \tau_f^{-1}(V_{dc}^* i_L)\right).
\end{aligned} \tag{18}$$

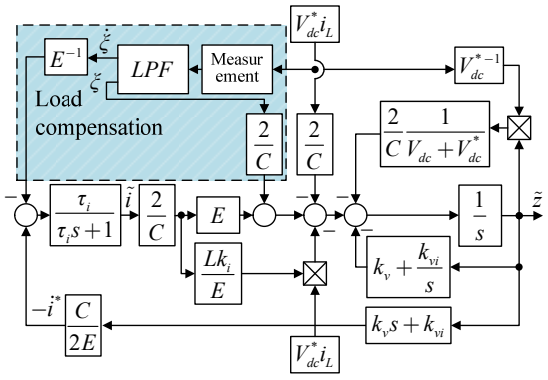

Fig. 3

From (18) it follows that $\lim\limits_{t\to\infty}\xi(t) = V_{dc}^* i_L$ in steady-state, providing disturbance compensation. On the other hand, load compensation given by (17) is open-loop and therefore should not have negative effect on system stability, even more for small τ_f with fast enough current loop, the disturbance rejection is fast as well [12]. The block-diagram of the closed-loop system is shown in Fig. 3.

Results of experimental and simulation investigation. The two sets of experimental tests were performed to show the effectiveness of the designed control algorithm with disturbance rejection capabilities. The first one for constant active current of the both directions supplied by current source inverter, developed in [11]. During second test, the DC-DC converter supplies highly dynamic electromechanical system based on vector controller IPMSM.

Constant load test. The experimental setup consists of a DC-DC converter powered by lithium-ion batteries $E = 54$ V, PWM frequency of 10 kHz with 2 μs "dead time" was set, $V_{dc}^* = 100$ V, $V_{dc}(0) = 54$ V. The positive load current 1 A was applied and removed at $t = 0.1$ s and $t = 0.2$ s, followed by the same regenerative load. Identical controller tuning is used for both control algorithms with and without disturbance compensation: $\tau_i = 1000$ rad/s, $k_v = 300$, $k_{vi} = k_v^2/4\,(\zeta_v = 1)$. $\tau_f = 0.005$ s, sampling time 100 μs. Note that in order to demonstrate effectiveness of the load current compensation, the sufficiently large time scale separation between control loops, equal to $\rho = 6.7$ is set.

The transients are shown in Fig. 4: *a* – controller (4), (6), (10) tuned at "symmetrical optimum" (experiment); *b*, *c* – controller with load compensation (4), (6), (17) (experiment and simulation). Comparison of experimental and simulation transients, shown in Fig. 4, demonstrates the effectiveness of the combined control technique applied: accuracy of voltage regulation has improved by almost an order of magnitude with

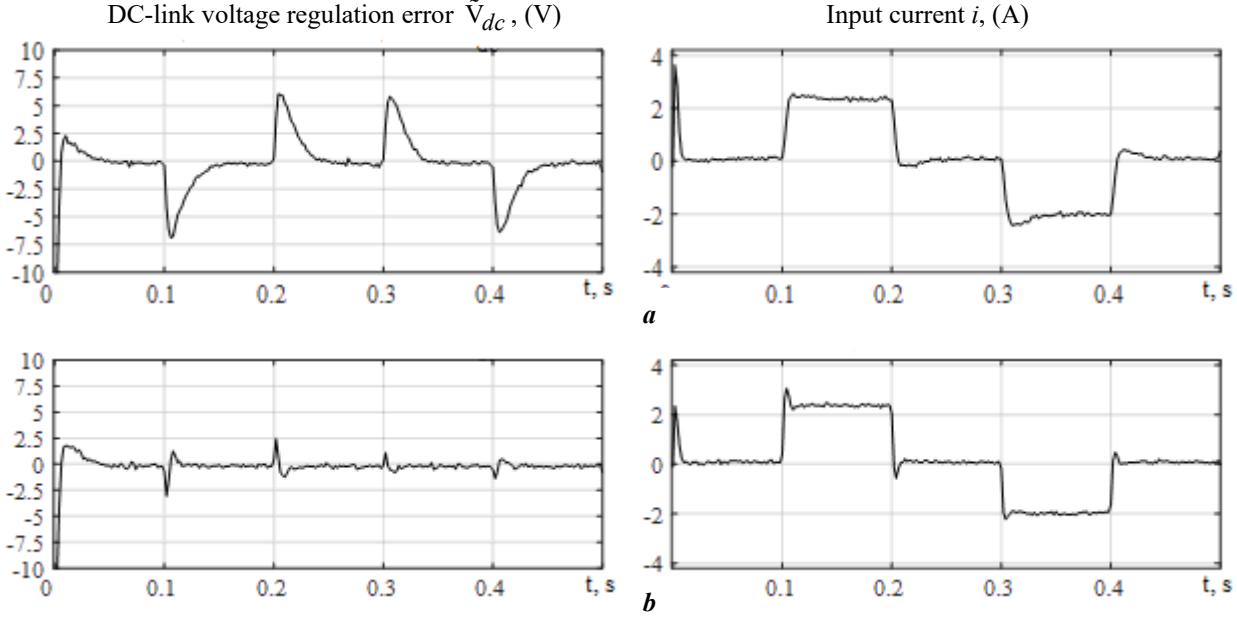

Fig. 4

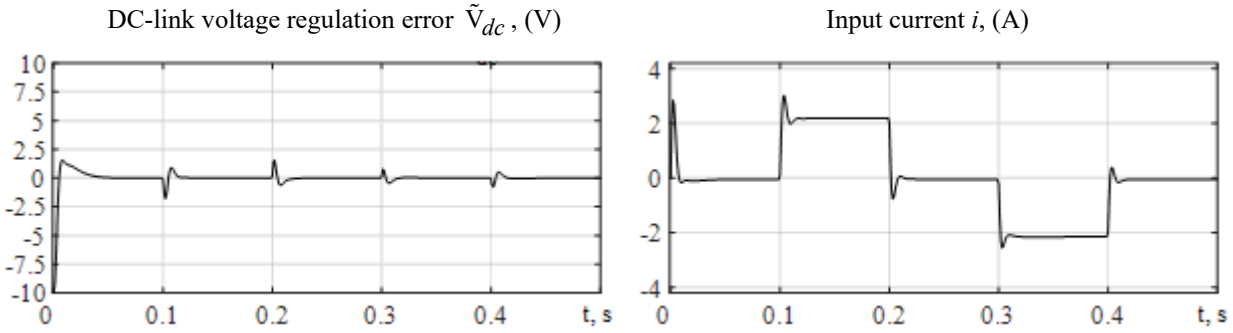

c

Fig. 4

no stability degradation. Although system dynamics is quite nonlinear, the voltage errors have small amplitude and are well-damped.

Dynamics of the composite system 'DC-DC converter – AC drive'. The simplified block-diagram of the tested electromechanical system based on vector controlled IPMSM is shown in Fig. 5. The DC-link of motor inverter is powered by the tested *DC-DC Converter.*

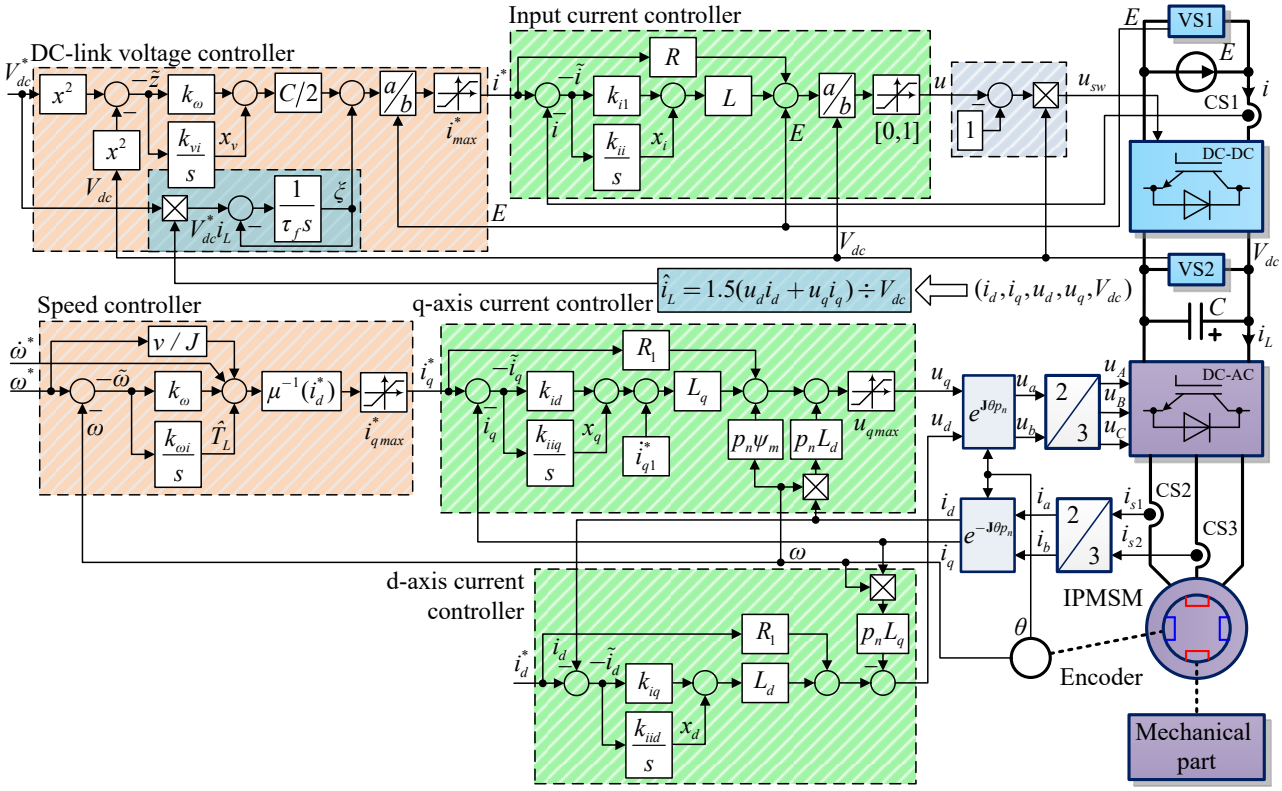

Fig. 5

Dynamics of the composite control system has been studied by simulation using the precomputed load current $\hat{i}_L$ based on the experimental transients from IPMSM speed control system test, shown in Fig. 5.

Note that DC-link voltage dynamics may be considered as decoupled from the motor dynamics due to compensation mechanism in PWM computation. In Fig. 5, (i_d, i_q), (u_d, u_q) are the stator currents and voltages in rotor oriented reference frame ($d-q$); ω is the rotor speed; ω^* is the speed reference; $\tilde{\omega} = \omega - \omega^*$ denotes speed tracking error; i_q^* is the q-axis reference current; VS1, VS2 and CS1 – CS3 are voltage and current sensors. For experimental and simulation tests the high dynamic performance speed tracking control algorithm has been used [13] with d-axis current reference set to zero.

The following operation sequence was applied to the IPMSM electric drive: 1) the unloaded motor is required to track the reference speed trajectory $\omega^*(t)$ with limited first and second time derivatives starting at $t = 0.1$ s from zero speed to 100 rad/s (45 % of rated) with the dynamic torque equal to the rated one (13.6 Nm); 2) from a time $t = 0.5$ s to $t = 1.3$ s a constant load torque equal to 75 % of the rated value is applied; 3) the motor decelerates starting from $t = 1.65$ s.

The simulation and experimental results of the speed trajectory tracking are shown in Fig. 6. As it follows from the transients, the simulation results match excellently the experimental data.

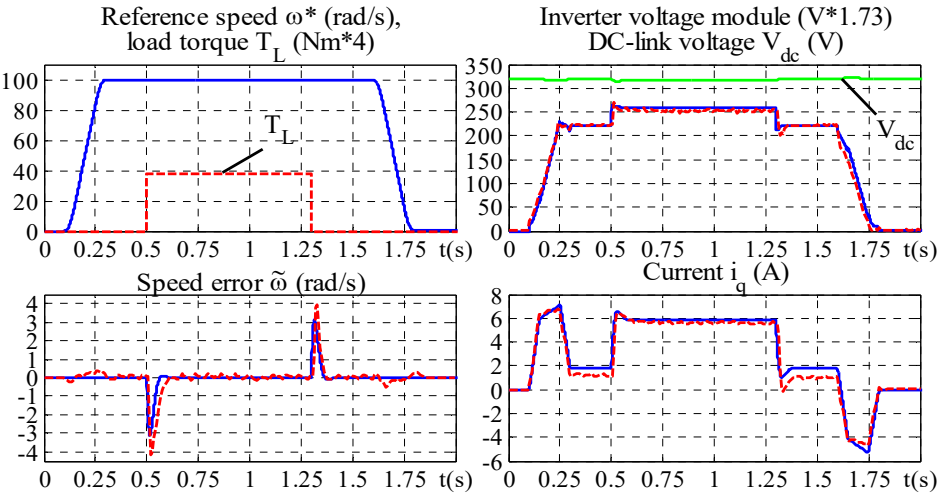

Fig. 6

During simulation test DC-DC converter feeds IPMSM drive which has the identical operating conditions as shown in Fig. 6. The estimated load current $\hat{i}_L$ is computed from the active power balance equation $V_{dc}\hat{i}_L = (3/2)(u_d i_d + u_q i_q)$. Input voltage is E = 130 V; reference voltage is $V_{dc}^* = 300$ V.

Transients, shown in Fig. 7 with red dashed lines, demonstrate the dynamic behavior of the DC-DC converter control system (4), (6), (10) with setting $k_v = 410$, $k_{vi} = k_v^2/2$, $k_i = 1800$ (ρ = 6.7) according to worst-case tuning. Blue lines in Fig. 7 illustrate transients of the DC-DC converter control system (Fig. 5) with additional disturbance compensation (17). During all test the significant improvement of voltage regulation accuracy is observed.

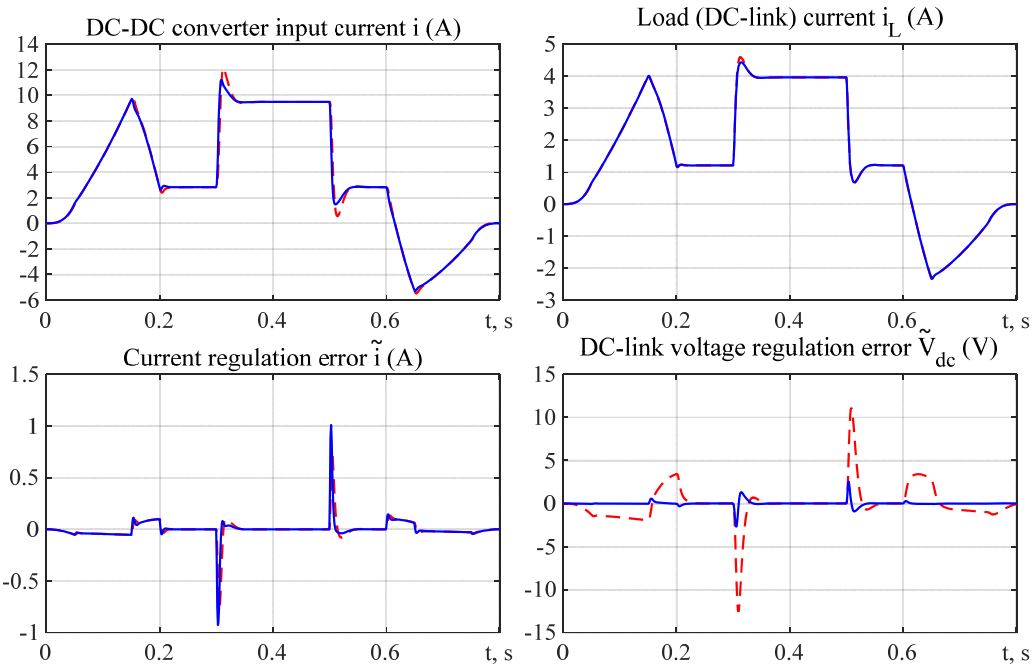

Fig. 7

Conclusions. This paper presents a novel control algorithm for of bidirectional DC-DC buck-boost power converters used as power supply for heavy duty dynamic loads such as high-performance vector-controlled IPMSM of electrical vehicles.

1. We propose a control algorithm, based on partial feedback linearization and linear PI voltage and current controllers, which forms the resulting system error dynamics of a special structure in the form of interconnected two linear asymptotically stable subsystems in a nonlinear feedback loop. Taking into consideration strong system nonlinearity and non-minimum phase nature, we use the linearized system analysis and the theory of cascaded systems with time-scale separation of processes in the control loops. The importance of such representation is that the resulting linearized system allows to define the load action not only as external disturbance but also assess its effect on the parameters of the closed-loop system. It is shown that in contrast to linear systems, external perturbation may lead to system potential instability, when current approaches the power balance limit. Mechanism of instability clearly indicates that controller parameters correction as function of load current is required to ensure stable operation and improved transient performance. We show that in case of heavy rapidly changing and bidirectional loads the effective way is 'worst-case' system tuning taking into account, for example, maximum phase margin of the frequency characteristic under different currents.

2. Based on designed cascaded structure, a disturbance rejection technique has been additionally applied to achieve remarkable improvement of voltage accuracy stabilization. As information for disturbance compensation, a direct measurement of load current can be used or estimation on the base of measurable variables as it is always possible in vector-controlled electrical drives. Since disturbance compensation is intrinsically an open-loop technique, the two technologies do not contradict each other. Essentially, only requirement is to limit rapid transients by adjusting the forming filter time constant. The reduction in voltage regulation errors achievable with such combined control has overall positive results on relaxing of converter nonlinearities effect.

The results of experiments and simulation study, including those based on experimental transients of the IPMSM drive, confirm the effectiveness of the proposed control system design and controllers tuning in terms of the dynamic performance and load capability of the converter. The studied electrical drive can be used in aerial and ground vehicles, gimbal suspensions, and multi-degree-of-freedom unanimous robots.

Acknowledgement. The authors acknowledge partial support from the National Science Foundation, US Office of Naval Research Global, and NATO. This material is based upon work supported by the National Science Foundation under Grant No. OISE-2415299, and under STCU Contract No. 7125. This research is funded by the NATO Science for Peace and Security (SPS) Programme under Grant G7925.

Disclaimer. Any opinions, findings, and conclusions or recommendations expressed in this material are those of the authors and do not necessarily reflect the views of the National Science Foundation, US Office of Naval Research Global, and NATO.

Appendix A. Rated parameters of the DC-DC converter: output capacitance C = 500 μF; inductance and resistance of the input circuit L = 11 mH, R = 0.5 Ohm.

Appendix B. The model of the IPMSM in rotor reference frame (d – q) is the following:

$$\begin{aligned}
&\dot{\theta} = \omega,\\
&\dot{\omega} = J^{-1}\left[1.5 p_n \left((L_d - L_q) i_d i_q + \psi_m i_q\right) - \nu\omega - T_L\right],\\
&\dot{i}_d = L_d^{-1}(-R_1 i_d + L_q p_n \omega i_q + u_d),\\
&\dot{i}_q = L_q^{-1}(-R_1 i_q - L_d p_n \omega i_d - \psi_m p_n \omega i_d + u_q),
\end{aligned} \tag{19}$$

where θ is the rotor angular position; ψ_m is the permanent magnets flux; T_L is the load torque; R_1 is the stator windings active resistance; L_d, L_q are the stator inductances; ν is the viscous friction coefficient; J is the total inertia; p_n is the pole pair number.

The speed control algorithm has been designed for $i_d^* = 0$. Controller guarantees asymptotic speed tracking if reference ω^* is smooth and bounded with bounded first $\dot{\omega}^*$ and second $\ddot{\omega}^*$ time derivatives.

Speed controller equations are given by:

$$\begin{aligned}
&i_q^* = \frac{1}{\mu}\left(\frac{\nu}{J}\omega^* + \dot{\omega}^* + \hat{T}_L - k_\omega \tilde{\omega}\right),\\
&\dot{\hat{T}}_L = -k_{\omega i}\tilde{\omega},
\end{aligned} \tag{20}$$

where $\tilde{\omega} = \omega - \omega^*$ is the speed tracking error; $\hat{T}_L$ is the estimate of the slowly varying load torque component T_L / J ; $\mu = 1.5 p_n \psi_m / J$; ($k_\omega = 100$, $k_{\omega i} = k_\omega^2 / 2$) are the proportional and integral gains of speed controller.

Current controllers are defined as:

$$\begin{aligned} u_q &= Ri_q^* + L_d p_n \omega i_d + \psi_m p_n \omega i_d + L_q\left(-k_{iq}\tilde{i}_q + x_q + i_{q1}^*\right), \\ \dot{x}_q &= -k_{iiq}\tilde{i}_q, \\ u_d &= Ri_d^* - L_q p_n \omega i_q + L_d\left(-k_{id}\tilde{i}_d + x_d\right), \\ \dot{x}_d &= -k_{iid}\tilde{i}_d, \end{aligned} \tag{21}$$

where ($k_{id} = k_{iq} = 1000$, $k_{iid} = k_{iiq} = k_{id}^2 / 4$) > 0 are proportional and integral gains of current controllers; $\tilde{i}_q = i_q - i_q^*, \tilde{i}_d = i_d - i_d^*$ are the errors;

$i_{q1}^* = \mu^{-1}(J^{-1}\nu\dot{\omega}^* + \ddot{\omega}^* + \dot{\hat{T}}_L) - \mu^{-1}k_\omega[-(k_\omega + J^{-1}\nu)\tilde{\omega} + \mu\tilde{i}_q + 1.5J^{-1}p_n(L_d - L_q)\tilde{i}_d i_q]$ is the known component of the time derivative of quadrature current reference.

Appendix C. Rated data of IPMSM NORD 100T2/4: power $P_r = 3$ kW; current $i_r = 5.4$ A (RMS); phase voltage $U_r = 385$ V (70 Hz supply); torque $T_r = 13.6$ Nm; speed $\omega_r = 220$ rad/s; stator resistance $R_1 = 1.7$ Ohm; $(d-q)$ inductances $L_d = 31$ mH, $L_q = 56$ mH; permanent magnets flux $\psi_m = 0.615$ Wb; viscous friction coefficient $\nu = 0.033$ Nm(rad/s)$^{-1}$; inertia $J = 0.0155$ kgm^2; pole pairs number $p_n = 2$.

1. Kapat S., Krein P.T. A tutorial and review discussion of modulation, control and tuning of high-performance DC-DC converters based on small-signal and large-signal approaches. *IEEE Open Journal of Power Electronics*. 2020. Vol. 1. Pp. 339-371. DOI: https://doi.org/10.1109/OJPEL.2020.3018311.
2. Gorji S.A., Sahebi H.G., Ektesabi M., Rad A.B. Topologies and control schemes of bidirectional DC-DC power converters: An overview. *IEEE Access*. 2019. Vol. 7. Pp. 117997-118019. DOI: https://doi.org/10.1109/ACCESS.2019.2937239.
3. Forouzesh M., Siwakoti Y.P., Gorji S.A., Blaabjerg F., Lehman B. Step-up DC-DC converters: A comprehensive review of voltage-boosting techniques, topologies, and applications. *IEEE Transactions on Power Electronics*. 2017. Vol. 32. No 12. Pp. 9143-9178. DOI: https://doi.org/10.1109/TPEL.2017.2652318.
4. Vasca F., Iannelli L. Dynamics and Control of Switched Electronic Systems: Advanced Perspectives for Modeling, Simulation and Control of Power Converters. Springer London, 2012. 494 p. DOI: https://doi.org/10.1007/978-1-4471-2885-4.
5. Sira-Ramirez H.J., Ramón S.O. Control Design Techniques in Power Electronics Devices. Springer London, 2006. 423 p. DOI: https://doi.org/10.1007/1-84628-459-7.
6. Sanders S.R., Noworolski J.M., Liu X.Z., Verghese G.C. Generalized averaging method for power conversion circuits. *IEEE Transactions on Power Electronics*. 1991. Vol. 6. No 2. Pp. 251-259. DOI: https://doi.org/10.1109/63.76811.
7. Vazquez S., Rodriguez J., Rivera M., Franquelo L.G., Norambuena M. Model predictive control for power converters and drives: Advances and trends. *IEEE Transactions on Industrial Electronics*. 2017. Vol. 64. No 2. Pp. 935-947. DOI: https://doi.org/10.1109/TIE.2016.2625238.
8. Mukherjee N., Strickland D. Control of cascaded DC-DC converter-based hybrid battery energy storage systems - part II: Lyapunov approach. *IEEE Transactions on Industrial Electronics*. 2016. Vol. 63. No 5. Pp. 3050-3059. DOI: https://doi.org/10.1109/TIE.2015.2511159.
9. Song Z., Hou J., Hofmann H., Li J., Ouyang M. Sliding-mode and Lyapunov function-based control for battery/supercapacitor hybrid energy storage system used in electric vehicles. *Energy*. 2017. Vol. 122. Pp. 601-612. DOI: https://doi.org/10.1016/j.energy.2017.01.098.
10. Peresada S., Kovbasa S., Pushnitsyn D., Zaichenko Y. Two nonlinear controllers for voltage source AC-DC converter. *IEEE First Ukraine Conference on Electrical and Computer Engineering (UKRCON)*. Kyiv, Ukraine, 2017. Pp. 462-467. DOI: https://doi.org/10.1109/UKRCON.2017.8100532.
11. Peresada S.M., Nikonenko Y.O., Kovbasa S.M., Kuznetsov A., Lukianchikov A.L. Design of cascaded voltage control systems of bidirectional DC-DC buck-boost converters. *Tekhnichna Elektrodynamika*. 2024. No 1. Pp. 27-37. DOI: https://doi.org/10.15407/techned2024.01.027. (Ukr)
12. Lyubchyk L. Inverse model approach to disturbance rejection problem. In: Advanced Control Systems: Theory and Applications. River Publishers, 2021. Pp. 129-166. DOI: https://doi.org/10.1201/9781003337010-6.
13. Peresada S., Nikonenko Y., Reshetnyk V., Kiselychnyk O. Dynamics of the synchronous motor based traction electromechanical systems with hybrid energy sources. *IEEE Problems of Automated Electrodrive. Theory and Practice (PAEP)*. Kremenchuk, Ukraine, 2020. Pp. 1-6. DOI: https://doi.org/10.1109/PAEP49887.2020.9240798.

УДК 621.314.1

КОМБІНОВАНЕ КЕРУВАННЯ ДВОНАПРАВЛЕНИМИ DC-DC ПЕРЕТВОРЮВАЧАМИ ДЛЯ ВИСОКОДИНАМІЧНИХ НАВАНТАЖЕНЬ

С.М. Пересада[1], докт. техн. наук, **Є.О. Ніконенко**[1], докт. філософ., **С.Е. Ляшевський**[2], професор
[1] **НТУ України «Київський політехнічний інститут ім. Ігоря Сікорського»,**
пр. Берестейський, 37, Київ, 03056, Україна, **e-mail:** sergei.peresada@gmail.com.
[2] **Рочестерський Технологічний Інститут,**
Рочестер, Нью-Йорк, США.

Роботу присвячено розробці каскадних систем керування напругою ланки постійного струму реверсивних силових DC-DC перетворювачів, які живлять високодинамічні навантаження, такі як векторно-керовані синхронні електроприводи. Новітні результати по розробці методів синтезу і аналізу керувань DC-DC перетворювачів, які є суттєво нелінійними та немінімально фазовими об'єктами, дали змогу не тільки синтезувати системи з підвищеними показниками якості керування, але й встановили невідомі раніше властивості, що важливі для їх подальшого вдосконалення і оптимізації. Показано, що струм навантаження діє не тільки як зовнішнє збурення, але й впливає на параметри замкненої системи і таким чином визначає показники якості керування та її стійкість. Задля послаблення впливу варіацій параметрів, обумовлених цим явищем, запропоновано використовувати комбіноване керування, яке містить: а) оптимізацію каскадної системи на 'симетричний' оптимум з налаштуванням виходячи з 'найгіршого випадку', що забезпечує заданий запас стійкості відносно максимального значення навантаження; б) компенсацію збурення на основі вимірювання або оцінювання струму навантаження. В той час як перша технологія покращує робастність відносно значень струмів, але зменшує динамічну точність, друга сприяє підвищенню точності стабілізації напруги. Для DC-DC перетворювачів, які живлять векторно-керовані синхронні двигуни з постійними магнітами (IPMSM), розрахунок навантаження здійснюється з рівняння балансу потужності системи «DC-DC перетворювач – електропривод». Композитна електромеханічна система забезпечує високі показники якості перехідних процесів DC-DC перетворювача разом з розширеним діапазоном навантаження, що підтверджується результатами експериментів, а також моделювання на основі експериментальних процесів синхронного електроприводу. Бібл. 13, рис. 7, табл. 1.

Ключові слова: DC-DC перетворювач, комбінований алгоритм керування, електропривод, регулятор напруги, стійкість, компенсація струму навантаження.

Received 23.03.2026
Accepted 31.03.2026